

# A NEW APPROACH FOR DETERMINING THE CURVATURE DUCTILITY OF REINFORCED CONCRETE BEAMS

Saeid FOROUGHI<sup>1\*</sup>, S. Bahadir YUKSEL<sup>1</sup>

## Abstract

*This paper presents a numerical parametric study of the moment-curvature and curvature ductility of doubly-reinforced beams with different parameters. The effects of the strength of the concrete and the amount of the reinforcement, including the tensile and compression reinforcement on the complete moment-curvature behavior and the curvature ductility factor of the beam sections, have been studied. A new predictive formula for the ductility factor of beam sections that considers the different parameters has been developed. In a continuation of the study, the flexural ductility of beams designed with different parameters according to the ductility factor proposed by different researchers was investigated. Based on the results of the numerical analysis, the proposed predictions for the curvature ductility factor were verified by comparisons with other predictive formulas. The proposed formula offers fairly accurate and consistent predictions for the curvature ductility factor of beam sections. It is shown that the concrete's compression strength and the amount of reinforcing steel, including the compression reinforcement ratios, have an effect on the curvature ductility factor of beam sections.*

## Address

<sup>1</sup> Dept. of Civil Engineering, Faculty of Engineering and Natural Sciences, Konya Technical University, Konya, Turkey

\* **Corresponding author:** saeid.foroughi@yahoo.com

## Key words

- Numerical analysis,
- Moment-curvature,
- Ductility,
- Flexural,
- Reinforced concrete beam,
- Reinforcement.

## 1 INTRODUCTION

Ductility can be defined as the ability of a material to undergo large deformations without any rupture before failure (Zareef and Madawy, 2018). The ductility of reinforced concrete (RC) beams is very important since it is essential to avoid the brittle failure of the structure by ensuring adequate curvature at the ultimate limit state (Arsalan and Cihanli, 2010). The ductility of RC beams is the property that allows structures to dissipate energy under seismic loading; consequently, the brittle failures of RC structures can be avoided (Haytham and Amar, 2017). The ductility performance of a RC member does not increase or decrease in direct proportion to the ductility of the concrete used; it is also dependent of other parameters such as the reinforcement details (Kwan et al., 2002). In the flexural design of RC beams, the strength and deformability, which are interrelated, need to be considered simultaneously.

However, in current design codes, the design of a beam's strength is separated from its deformability, and an evaluation of its deformability is independent of some key parameters, such as the concrete's strength, the steel's yield strength, and the confinement content (Adari, 2017). Several researchers (Bai and Au, 2011; Ho et al., 2004; Debernardi and Taliano, 2002; Pecce and Predictions, 1999) have reported that the values of the curvature ductility for beam sections with normal and high strength concrete are different. Also, it has been determined that the flexural ductility of RC beam sections is dependent not only on the amount of the reinforcement, including the compression reinforcement, but also on the concrete's compressive strength and the steel's yield strength (Lee, 2013).

The factors affecting the nonlinear behavior of RC beams are the tensile and compression reinforcement ratio and the compressive strength of the concrete. The aim of this study is to examine

the effects of factors such as the tensile reinforcement ratio, the compression reinforcement ratio, and the concrete's compressive strength, which affect the moment- curvature relationships and ductility of RC beam sections. Rectangular beam section models with an equal cross-sectional area having different parameters were designed. In this study, the effects of the concrete's compression strength, and the amount of reinforcement, including the tensile and compression reinforcement, on the complete moment-curvature and the curvature ductility factor of doubly-reinforced beams have been evaluated. A new predictive formula for the curvature ductility factor of doubly-reinforced beam sections that considers the different parameters has been developed. In a continuation of the study, the flexural ductility of doubly-reinforced beam models designed with different parameters according to the relations proposed by different researchers was investigated analytically. The final results obtained were examined by comparing them according to different parameters and models.

## 2 FLEXURAL DUCTILITY OF REINFORCED CONCRETE BEAMS

In the case of a flexural member, its sectional ductility based on the curvature and/or the member's ductility based on deflection is usually considered (Park and Paulay, 1975). Moment- curvature relationships are a useful resource for the solution of a variety of inelastic and geometrically non-linear structural problems involving elements under a combined axial load and bending (Liew, 2017; Simao et al., 2016). Determining the moment and curvature response of a cross-section is an important step in fulfilling strength and serviceability design requirements (Dhakal and Moustafa, 2019). Yield moment ( $M_y$ ), ultimate moment ( $M_u$ ), yield curvatures ( $\varphi_y$ ), ultimate curvatures ( $\varphi_u$ ) and curvature ductility ( $\mu_\varphi$ ) values are calculated from the moment-curvature relationships. The curvature ductility factor is obtained by the ratio between the curvature determined at the ultimate limit state and the curvature determined at the first yield ( $\mu_\varphi = \varphi_u / \varphi_y$ ).

### 2.1 Previous Research on the Curvature Ductility Factor

A considerable amount of studies on the ductility and flexural behavior of normal and high- strength concrete elements under a static load can be found in the literature (Lee, 2013; Au et al., 2011; Bai and Au, 2011; Arslan and Cihanli, 2010; Lam et al., 2009a, 2009b; Jang et al., 2008; Rashid and Mansur, 2005; Ho et al., 2004). The ultimate states in each research work are defined in different forms. In this part of the study, the flexural ductility of doubly-reinforced beam models designed with different concrete strengths and compression and tensile strength ratios according to the relations proposed by the different researchers was investigated analytically. The bending ductility of doubly-reinforced beams was obtained by using the relations suggested from (Lee, 2013; Kwan and Ho, 2010; Kwan et al., 2002; Pam et al., 2001a, 2001b). The equations defining the curvature ductility of doubly-reinforced beam elements are summarized below. Pam et al., (2001a) derived the predictive equation (1) based on the results of designing beam sections with the concrete strength  $f_{cc}$  from 30MPa to 100MPa, a steel yield strength  $f_y = 400\text{--}460\text{MPa}$ , the tensile reinforcement ratio  $\rho'$  from 1%–5%, and the compression

reinforcement ratio  $\rho'$  from 0%–1.5%. The ductility factor has been correlated with the concrete grade, and the tensile and compression steel ratios by regression analysis; the following formula is given for a direct evaluation of the flexural ductility derived:  $\rho$  is the tensile reinforcement ratio;  $\rho_b$  is the balanced reinforcement ratio;  $\rho'$  is the compression reinforcement ratio; and  $f_{ck}$  is the concrete compressive strength:

$$\mu = 10.7(f_{ck})^{-0.45} [(\rho - \rho') / \rho_b]^{-1.25} \times [1 + 95.2(f_{ck})^{-1.1} (\rho' / \rho)^3] \quad (1)$$

Replacing the last term in Equation (1) by unity, a simplified equation (2) for the ductility factor was proposed by Kwan et al. (2002):

$$\mu = 10.7(f_{ck})^{-0.45} [(\rho - \rho') / \rho_b]^{-1.25} \quad (2)$$

Kwan and Ho (2010) obtained the  $\mu$  values that are correlated to the various structural parameters using regression analysis to produce Equation (3) to enable a direct evaluation of the flexural ductility of beams without conducting any nonlinear moment-curvature analysis. In Equation (3),  $\lambda$  is the degree of reinforcement, and  $f_r$  is the confining compression. Herein, the degree of reinforcement is denoted by  $\lambda$  and explicitly defined as  $\lambda = (\rho - \rho') / \rho_b$ . In order to study the effects of the various structural parameters, i.e.,  $f_{ck} = 40\text{--}100\text{MPa}$ ,  $f_y = 250\text{--}600\text{MPa}$ ,  $f_r = 0\text{--}4\text{MPa}$ ,  $\rho' = 0\text{--}2\%$ , and  $\rho = 0.4\rho_b - 2\rho_b$  are considered:

$$\mu = 10.7m(\lambda)^{-1.25n} (f_{ck})^{-0.45} (f_y / 460)^{-0.25} \quad (3)$$

$$m = 1 + 2.5(f_{ck})^{-0.5} (f_r / f_{ck}), \quad n = 1 + 5.0(f_r / f_{ck})$$

Lee (2013) studied the effects of concrete strength, steel yield strength, and the amount of reinforcement, including compression reinforcement on the complete moment-curvature behavior and the curvature ductility factor of doubly-reinforced beam sections. For the parametric study,  $f_{ck} = 30\text{--}100\text{MPa}$  to cover both normal and high-strength concretes,  $f_y = 300\text{--}600\text{MPa}$ ,  $E_s = 2 \times 10^5\text{MPa}$ ,  $\rho = 0.1\rho_b\text{--}\rho_b$  and  $\rho' = \rho$  are considered. In doubly-reinforced beam sections, considering the influence of parameters such as the material strength, reinforcement ratio, and stress of the compression reinforcement, the predictive equation of the curvature ductility factor can be offered based on the previous parametric study as Equation (4).  $f_{sc}$  is the stress of the compression reinforcement, which is calculated at the ultimate stage (Lee, 2013).

$$\mu_\varphi = \left[ \left( \rho - \rho' \frac{f_{sc}}{f_y} \right) / \rho_b \right]^{-1.283} (f_y)^{-0.230} [-0.6(f_{ck})^2 + 95.2(f_{ck}) + 2506.2] \times 10^{-3} \quad (4)$$

$$\theta_p = (\varphi_u - \varphi_c) L_p = \left[ \varphi_u - \left( \frac{M_u}{M_y} \right) \varphi_y \right] L_p$$

## 3 PLASTIC ANALYSIS FOR BEAMS

Methods based on a plastic analysis should only be used for the inspection at the ultimate limit state. The ductility of the critical sections should be sufficient for the envisaged mechanism to be formed. The plastic analysis should be based either on the lower bound (static) method or on the upper bound (kinematic) method. Plastic analysis without any direct inspection of the rotation capacity may be used for the ultimate limit state if the conditions

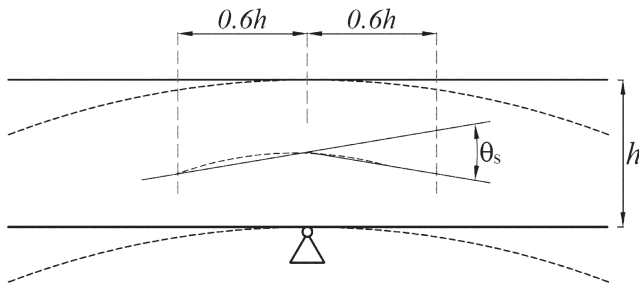


Fig. 1. Plastic rotation ( $\theta_s$ ) of reinforced concrete sections for continuous beams (Eurocode 2, 2004; Model Code, 2010)

of the ductility of the critical sections are met (Eurocode 2, 2004; Model Code, 2010).

### 3.1 Rotation Capacity

The simplified procedure for continuous beams is based on the rotation capacity of the beam over a length of approximately 1.2 times the depth of the section. It is assumed that these zones undergo plastic deformation (formation of yield hinges) under the relevant combination of actions. The verification of the plastic rotation in the ultimate limit state is considered to be fulfilled if it is shown that under the relevant combination of actions, the calculated rotation,  $\theta_s$ , is less than or equal to the allowable plastic rotation (Fig. 1).

In the region of yield hinges,  $x_u/d$  should not exceed the value of 0.45 for concrete strength classes less than or equal to C50/60 and 0.35 for concrete strength classes greater than or equal to C55/67.  $x_u$  is the neutral axis depth, and  $d$  is the effective depth of a cross-section. The rotation  $\theta_s$  should be determined on the basis of the design values for the actions and materials and on the basis of the mean values for prestressing at the relevant time. In the simplified procedure, the allowable plastic rotation may be determined by multiplying the basic value of the allowable rotation ( $\theta_{pl,d}$ ) by correction factor  $k_\lambda$ , which depends on the shear slenderness. The recommended values for steel Classes B and C and concrete strength classes less than or equal to C50/60 and C90/105 are given in Fig. 2 (the values apply to a shear slenderness of  $\lambda=3.0$ ). The values for concrete strength classes C 55/67 to C 90/105 may be interpolated accordingly. The values apply for a shear slenderness,  $\theta_{pl,d}$  should be multiplied by  $k_\lambda = \sqrt{\lambda/3}$ , where  $\lambda$  is the ratio of the distance between the zero point and the maximum moment after redistribution. As a simplification,  $\lambda$  may be calculated for the concordant design values of the bending moment and shear ( $\lambda = M_{sd}/(V_{sd} \cdot d)$ ) (Eurocode 2, 2004; Model Code, 2010).

The plastic hinge rotation ( $\theta_p$ ), of RC beams depends on a number of parameters, including the definition of the yielding and ultimate curvatures, section geometry, material properties, tension and compression reinforcement ratios, transverse reinforcement, cracking and tension stiffening, the stress-strain curve for the concrete, the stress-strain curve for the reinforcement, the bond-slip characteristics between the concrete and the reinforcing steel, the support conditions and the magnitude and type of loading, the axial force, the width of the loading plate, the influence of the shear, and the presence of a column. The moment-curvature relationship of a typical beam subjected to a uniform load are shown in Fig. 3. It is recommended to estimate the plastic rotational capacity that

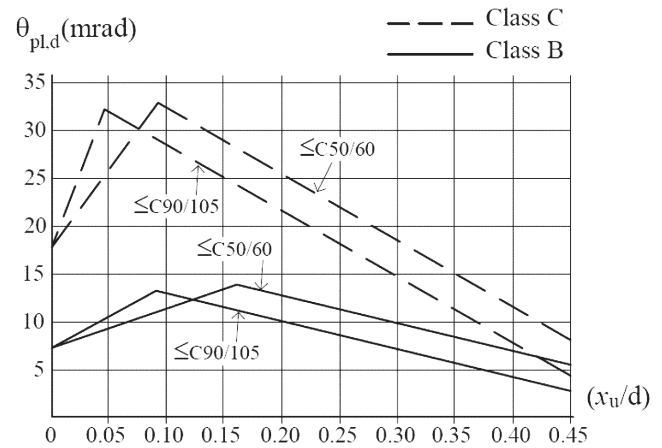


Fig. 2 Basic value of the allowable rotation ( $\theta_{pl,d}$ ), of the reinforced concrete sections for Class B and C reinforcements (Eurocode 2, 2004; Model Code, 2010)

can be achieved at potential plastic hinge sections by utilizing the moment-curvature relationships of the sections. The value of the plastic hinge rotation at the ultimate stage can be easily calculated by the following Equation (5), where  $\varphi_u$  refers to the maximum curvature, and  $\varphi_y$  refers to the yield curvature, as shown in Fig. 3. The length of the plastic deformation region, which is called the plastic hinge length ( $L_p$ ), is taken as half of the section length in the active direction ( $L_p = 0.5h$ ).

$$\theta_p = (\varphi_u - \varphi_e) L_p = \left[ \varphi_u - \left( \frac{M_u}{M_y} \right) \varphi_y \right] L_p \quad (5)$$

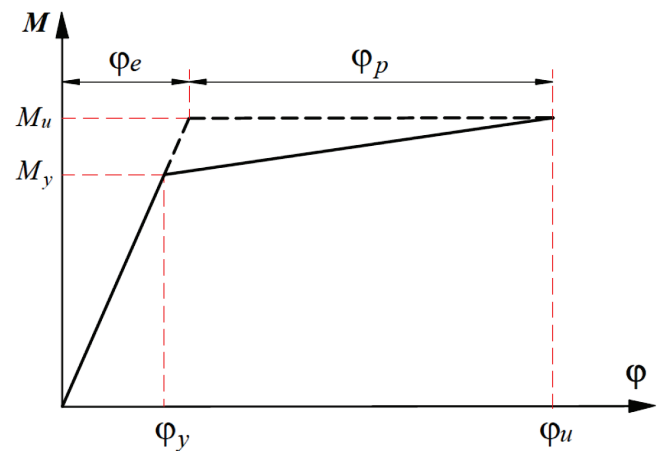


Fig. 3 Moment-curvature relationship for reinforced concrete beams

## 4 MATERIALS AND METHOD

Many variables influence the curvature ductility with the nonlinear behavior of RC beams, and the numerical analysis presented was performed on models designed by considering variable parameters. The effect of the different parameters was studied by varying one parameter at a time and keeping the value of the other parameters fixed. The summary of the designed RC beam cross-section properties is given in Tab. 1. A typical beam section has a width of  $b_w = 300\text{mm}$ , and a total depth of  $h = 600\text{mm}$  was designed. The compression and tensile reinforcement is provided at depth  $d' = 50\text{mm}$  and  $d = 550\text{mm}$  ( $d = h - d'$ ) from the top, respectively. For all the

RC members, C25, C30, C35, C40, C45 and C50 were chosen as the concrete grade, and B420C was selected as the reinforcement for the reinforcement behavior model. Concrete with a strength lower than C25 cannot be used in all RC buildings to be built within the scope of the Turkish Building Earthquake Code (TBEC, 2018) regulations. In moment-curvature analyses, the material models given in Tab. 2 were used for the unconfined concrete and reinforcement steel. Due to its insignificant effect, the tensile strength of the concrete has been ignored in the moment-curvature analyses.

The most important issue to be considered when calculating and designing an RC beam section is to ensure that the reinforcement ratio obtained is smaller than the balanced reinforcement ratio. The limit values given in TS500 (2000) are taken into consideration in this study. The ratio of the tensile reinforcement ( $\rho$ ) in the beams should not be less than the minimum values given in Equation (6). In TS500 (2000), the reinforcement ratio is limited to Equation (7) in order to provide ductile behavior in the RC beams. The ratio of the tensile reinforcement in the RC beams should not be more than the maximum value given in Equation (7) and not more than 2%. The difference between the tensile and compression reinforcement ratios in the beams should not exceed 0.85 of the balanced reinforcement.

$$\rho = \frac{A_s}{b_w d} \geq \rho_{\min} = 0.8 \frac{f_{ctd}}{f_{yd}} \quad (6)$$

$$(\rho - \rho') \leq \rho_{\max} = 0.85 \rho_b$$

$$\rho_b = 0.85 k_1 \left( \frac{f_{ctd}}{f_{yd}} \right) \left( \frac{700}{700 + f_{yd}} \right) \quad (7)$$

The  $k_1$  value is provided should not be less than 0.70 and not greater than 0.85 (TS500, 2000).

$$k_1 = 0.85 - 0.006(f_{ck} - 25) < 0.85; f_{ck} > 25 \text{ MPa} \quad (8)$$

$$k_1 = 0.85 \quad ; f_{ck} \leq 30 \text{ MPa}$$

A total of 66 RC beam models with different concrete strengths and different tensile and compression reinforcement ratios have been designed (Tab. 1). The provisions in TBEC (2018) and TS500 (2000) have been taken into consideration in the design of the RC beam models. In the RC beam models designed in different parameters, i.e.,  $\rho_{\max} = 0.85 \rho_b$  as the ratio of tensile reinforcement and the values of  $\rho' = 0.0, 0.1 \rho_{\max}, 0.2 \rho_{\max}, 0.3 \rho_{\max}, 0.4 \rho_{\max}, 0.5 \rho_{\max}, 0.6 \rho_{\max}, 0.7 \rho_{\max}, 0.8 \rho_{\max}, 0.9$ , and  $\rho_{\max}$ , as the compression reinforcement ratio are taken into account. In the RC beam models, six different concrete classes i.e., C25, C30, C35, C40, C45 and C50 were taken into account. In the beam models, the tensile reinforcement ratio for each concrete strength was kept constant with  $\rho_{\max} = 0.85 \rho_b$ . By changing the compres-

**Tab. 1** Details for the RC beam cross-sections designed

$\rho'/\rho$	Material: C25		Material: C30		Material: C35		Material: C40		Material: C45		Material: C50	
	$\rho$	$\rho'$										
<b>0.0</b>		0.0		0.0		0.0		0.0		0.0		0.0
<b>0.1</b>		0.0018		0.0021		0.0024		0.0026		0.0028		0.0030
<b>0.2</b>		0.0037		0.0043		0.0048		0.0053		0.0057		0.0061
<b>0.3</b>		0.0055		0.0064		0.0072		0.0079		0.0085		0.0091
<b>0.4</b>		0.0074		0.0085		0.0096		0.0105		0.0114		0.0121
<b>0.5</b>	0.0184	0.0092	0.0213	0.0107	0.0240	0.0120	0.0263	0.0132	0.0285	0.0142	0.0303	0.0152
<b>0.6</b>		0.0111		0.0128		0.0144		0.0158		0.0171		0.0182
<b>0.7</b>		0.0129		0.0149		0.0168		0.0184		0.0199		0.0212
<b>0.8</b>		0.0147		0.0171		0.0192		0.0211		0.0228		0.0243
<b>0.9</b>		0.0166		0.0192		0.0216		0.0237		0.0256		0.0273
<b>1.0</b>		0.0184		0.0213		0.0240		0.0263		0.0285		0.0303

**Tab. 2** Material parameters for the concrete and reinforcement (TBEC, 2018)

Standard Strength	Parameters	Values
Concrete: C25-C50	Strain at maximum stress of unconfined concrete ( $\varepsilon_{co}$ )	0.002
	Ultimate compression strain of concrete ( $\varepsilon_{cu}$ )	0.0035
	Characteristic standard value of concrete compressive strength ( $f_{ck}$ )	25-50MPa
	Yield strain of reinforcement ( $\varepsilon_{y}$ )	0.0021
Reinforcement: B420C	Strain hardening value of reinforcing steel ( $\varepsilon_{sp}$ )	0.008
	Strain in reinforcing steel at ultimate strength ( $\varepsilon_{su}$ )	0.08
	Characteristic yield strength of reinforcement ( $f_{yk}$ )	420MPa
	Ultimate strength of reinforcement ( $f_{su}$ )	550MPa

sion reinforcement ratios, the moment-curvature relation of the RC beams were obtained. The analytically investigated parameters were calculated from different relations and moment-curvature relationships. Events such as how the stiffness and strength of the sections change and the ductility state of the cross-sectional behavior can also be observed through the moment-curvature relationship. The moment-curvature relationship is essential for the inelastic analysis of structures to predict section strengths, flexural stiffness, and section ductility. For the moment-curvature relations, SAP2000 software [20] was used to consider the different parameters. The curvature ductility was calculated from the established moment-curvature relationships. The major factors affecting the curvature ductility of a doubly-reinforced beam section were investigated. In the continuation of the study, a new predictive formula for the curvature ductility factor of the dou-

bly-reinforced beam sections has been developed considering the different parameters. Based on the numerical analysis results, the proposed predictions for the curvature ductility factor were verified by comparisons with other predictive formulas.

## 5 RESEARCH FINDINGS AND DISCUSSION

### 5.1 Nonlinear Moment-Curvature Analysis

In this part of the study, the moment-curvature relations of the RC beam elements designed with different parameters were obtained, and the curvature ductility was calculated. The moment-curvature relationships were obtained by SAP2000 software, which takes the nonlinear behavior of materials into consider-

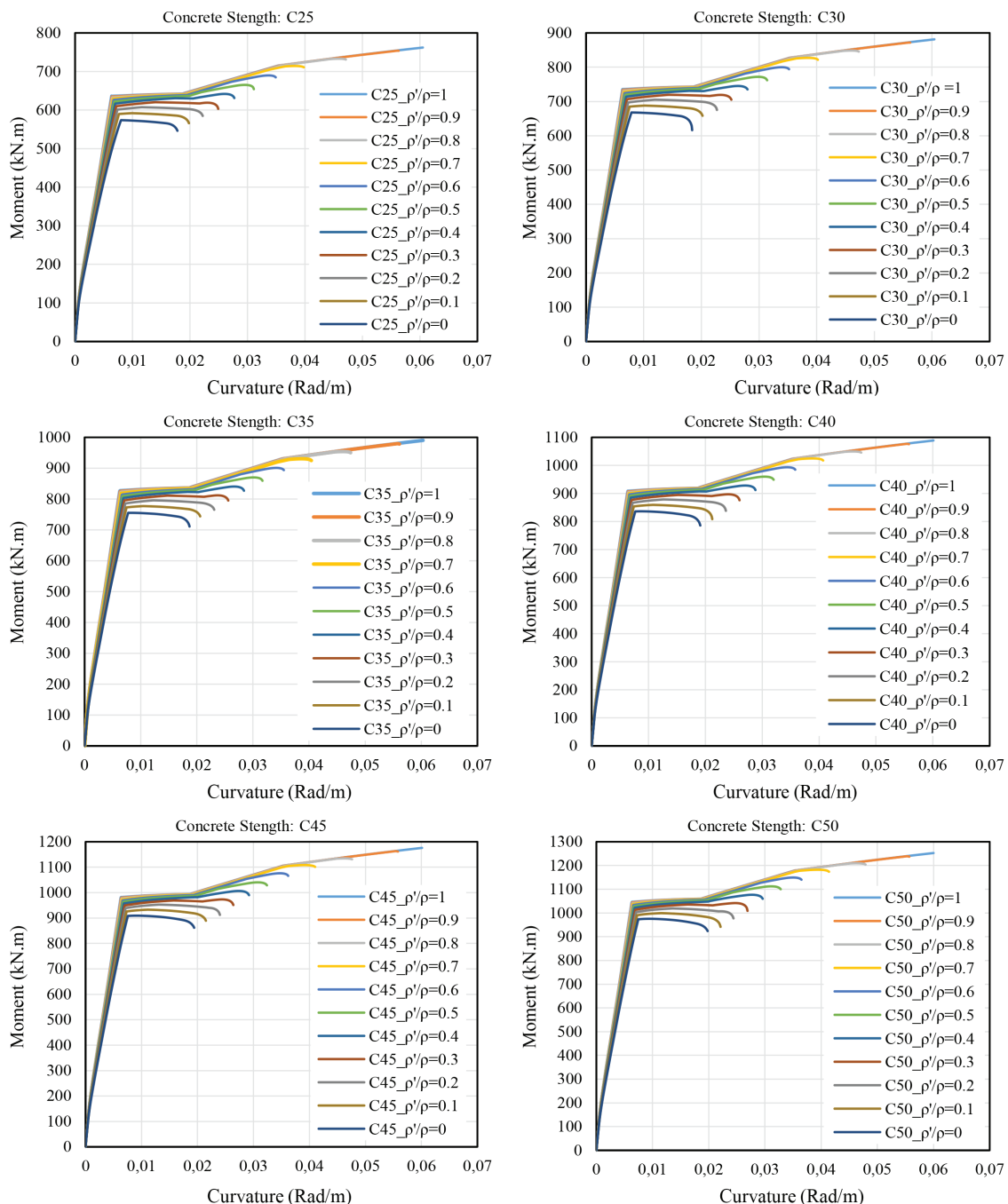


Fig. 4 Comparative moment-curvature relations for doubly-reinforced beam sections with different concrete strengths and reinforcement ratios

ation. The moment-curvature relationships of the rectangular RC beams for different longitudinal reinforcements (tensile and compression) and concrete strengths were obtained. The behavioral effects of the parameters examined were evaluated by the curvature ductility and moment-carrying capacity of the cross-section. The moment-curvature relationships obtained from the analytical results are presented in graphic form. The essential factors influencing the local ductility of the RC beams are the concrete strength, the yield strength of the steel, and the ratio of the tensile and compression reinforcement ( $\rho$  and  $\rho'$ ). A comparison of the moment-curvature relationships of the RC beams for different concrete strengths, i.e.,  $\rho'/\rho$ , is given in Fig. 4. The effect of the  $\rho'/\rho$  and concrete strength on the yield, ultimate moment, and curvature are given in Figs. 5 and 6. Since the maximum value of the axial load in the RC beams is limited to  $N = 0.10A_c f_c$ ,  $N = 0$  is considered in these analyses.

With the increase in the compression reinforcement ratio for the constant compressive strength of the concrete and tensile reinforcement ratio in the RC beams, the yield moment, ultimate moment, and ultimate curvature values obtained from the moment-curvature relationships increase, but the yield's curvature values decrease. With the increase in the compression reinforcement ratio, the maximum moment carrying capacity and ductility of the beam sections increase. It can be seen that the tensile reinforcement ratio for the RC beam sections basically affects both the shape of the moment-curvature curve and the ductility of a beam section. With the increase in the concrete's compressive strength in the RC beams with the constant compression and tensile reinforcement ratio, the yield and ultimate moment values increase.

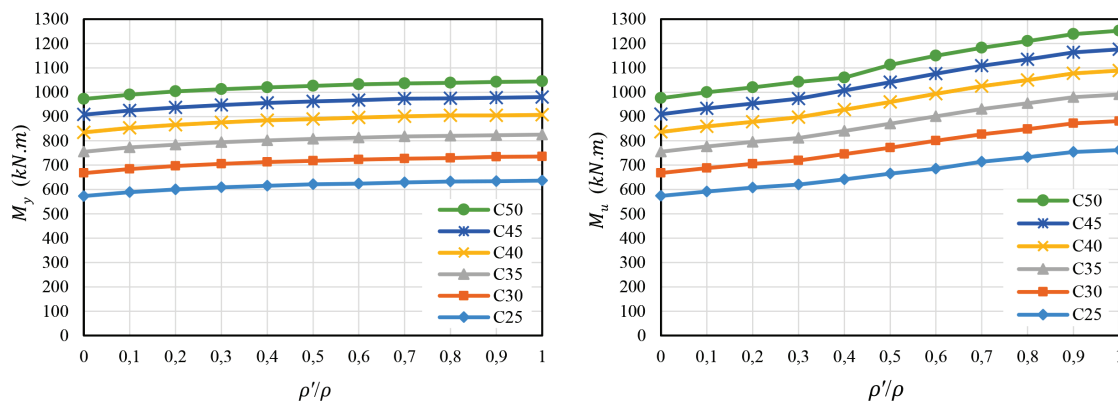


Fig. 5 Effect of  $\rho'/\rho$  and the concrete's strength on the yield and ultimate moment

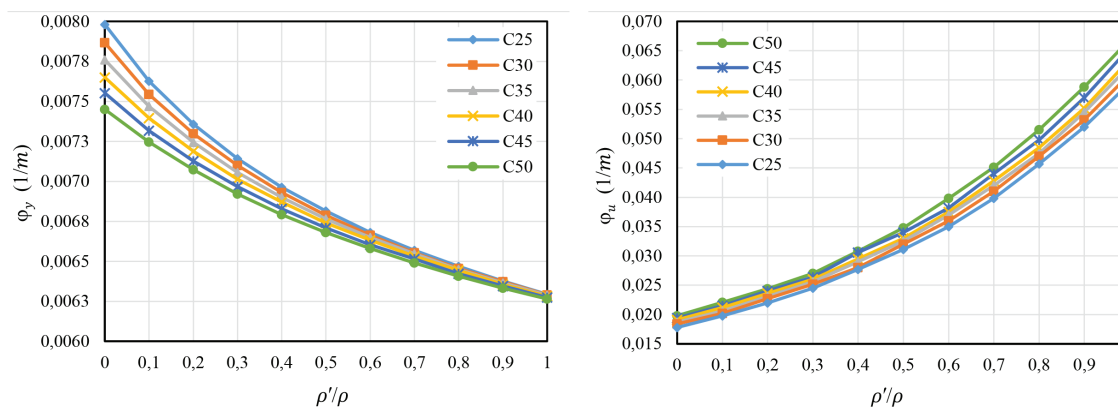


Fig. 6 Influence of  $\rho'/\rho$  and the concrete's strength on the yield and ultimate curvature

## 5.2 Plastic Rotation Capacity of Reinforced Concrete Beams

The plastic rotation capacity that can be achieved in the plastic hinge regions of reinforced concrete beams is calculated from the moment-curvature relations of the sections, according to the relations defined in Eurocode 2 (2004) and Model Code (2010). In order to calculate the rotational capacity of the RC beams, moment and curvature values were obtained from the moment-curvature relations by considering the non-linear behavior of the materials (Equation 5). By using the values recommended for the reinforcement and concrete strength classes in Eurocode (2004) or Model Code (2010), the rotation capacity values were obtained and compared with the values calculated from Equation (5). The rotation capacity values suggested in Eurocode (2004) or Model Code (2010) can be calculated according to the ultimate neutral axis depth and the effective depth of the cross-section values. A comparison of the rotational capacities of the plastic hinges calculated from the moment-curvature relations and according to Eurocode 2 (2004) are shown in Fig. 7.

The analytical results for the 66 RC beams with different tensile and compressive reinforcement ratios are compared with the various formulations given in Eurocode (2004), and calculated from the non-linear behavior relationships of the beams. According to the results obtained from the non-linear behavior of the RC beams, it was concluded that the reinforcement index and the concrete compressive strength have a significant effect on the plastic hinge's rotation capacity ( $\theta_p$ ). The plastic rotation capacity value increases with the increase in the  $\rho'/\rho$  ratio and concrete compressive strength. With the increase in the  $\lambda = (\rho - \rho')/\rho_b$  value, the plastic rotation capacity value

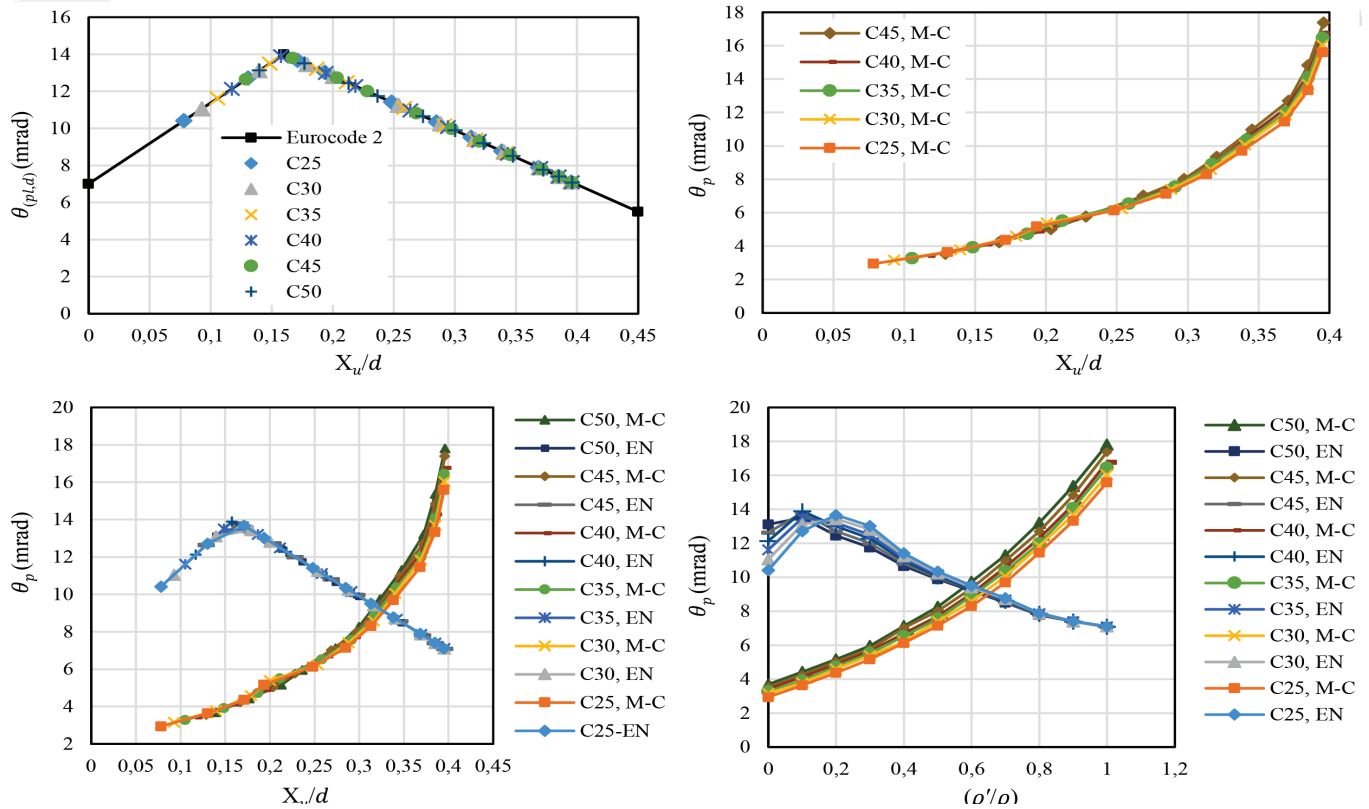


Fig. 7 Comparison of the rotational capacities of plastic hinges calculated from the moment- curvature relations and according to Eurocode 2 (2004)

decreases. With the increase of  $X_u/d$  value, the plastic rotation capacity value increases.

In Eurocode 2 (2004) or Model Code (2010), limit values are defined for the allowable plastic hinge capacity of RC elements according to different steel classes and concrete strength classes. In the simplified procedure, the allowable plastic rotation may be determined by multiplying the basic value of the allowable rotation ( $\theta_{pl,d}$ ) by a correction factor ( $k_\lambda$ ) that depends on the shear slenderness. For B class reinforcement and  $f_{ck} \leq 50\text{MPa}$ , when the  $x_u/d$  value is zero, the  $\theta_{pl,d}$  value is 7. It can be calculated as  $\theta_{pl,d} = 14$  for  $x_u/d = 0.16$  and  $\theta_{pl,d} = 5.5$  for  $x_u/d = 0.45$ . The limit values are defined for normal strength and high strength concrete.

In this study, since the concrete strength class is less than 50MPa, the plastic rotation capacity value calculated according to Eurocode 2 (2004) does not change. Since the reinforcement class is fixed in the reinforced concrete beams, the plastic rotation capacity value can still be calculated as constant. The change in the tensile reinforcement ratio, compression reinforcement ratio, and concrete compressive strength in the RC beams affects the plastic rotation values due to their effect on the neutral axis depth in the sections. As can be seen from the comparison of the results obtained, the plastic rotation values calculated according to the values obtained from the nonlinear behaviors are affected by all the design parameters. The values calculated according to Eurocode 2 (2004) or Model Code (2010) are greatly affected by the neutral axis depth and effective depth of a cross-section.

### 5.3 Curvature Ductility Obtained from the Moment-Curvature

Fig. 8 shows the relation of the curvature ductility ( $\mu_\phi$ ) for the doubly-reinforced beam sections with different compression

reinforcement ratios and concrete compressive strengths. In the RC beams, with the increase in the compression reinforcement ratio for the concrete’s constant compressive strength and tensile reinforcement ratio, the curvature ductility values calculated from the moment-curvature relationships increase. Under the same tensile and compression reinforcement ratios, the curvature ductility almost linearly decreases with the increased concrete compressive strength. This indicates that the ductility of the doubly-reinforced beam sections increases with an increase in the compression reinforcement ratios. The compression reinforcement ratio in the section of a doubly-reinforced beam has certain effects on the moment-curvature relations and ductility of the RC beam sections.

### 5.4 Derivation of an Alternative Curvature Ductility Equation for a Doubly-Reinforced Beam

From the results of the numerical analyses, the essential factors influencing the ductility of doubly-reinforced beams are  $f_{ck}$ ,  $\rho$  and  $\rho'$ . In the doubly-reinforced beams, the effect of  $f_{ck}$  has been found to be dependent on the amounts of  $\rho$  and  $\rho'$ , which determine the degree of reinforcement ( $\lambda = (\rho - \rho')/\rho_b$ ) of the section. Thus, based on the numerical analyses results, it can be observed that the use of the two significant variables  $\lambda$  and  $f_c$  should be incorporated to develop an alternative equation for the curvature ductility of doubly-reinforced beam sections. The basic formation of the curvature ductility factor equation for doubly-reinforced beams can be expressed as follows:

$$\mu_\phi = f \left\{ \left( \lambda = \frac{(\rho - \rho')}{\rho_b} \right), f_{ck} \right\} \tag{9}$$

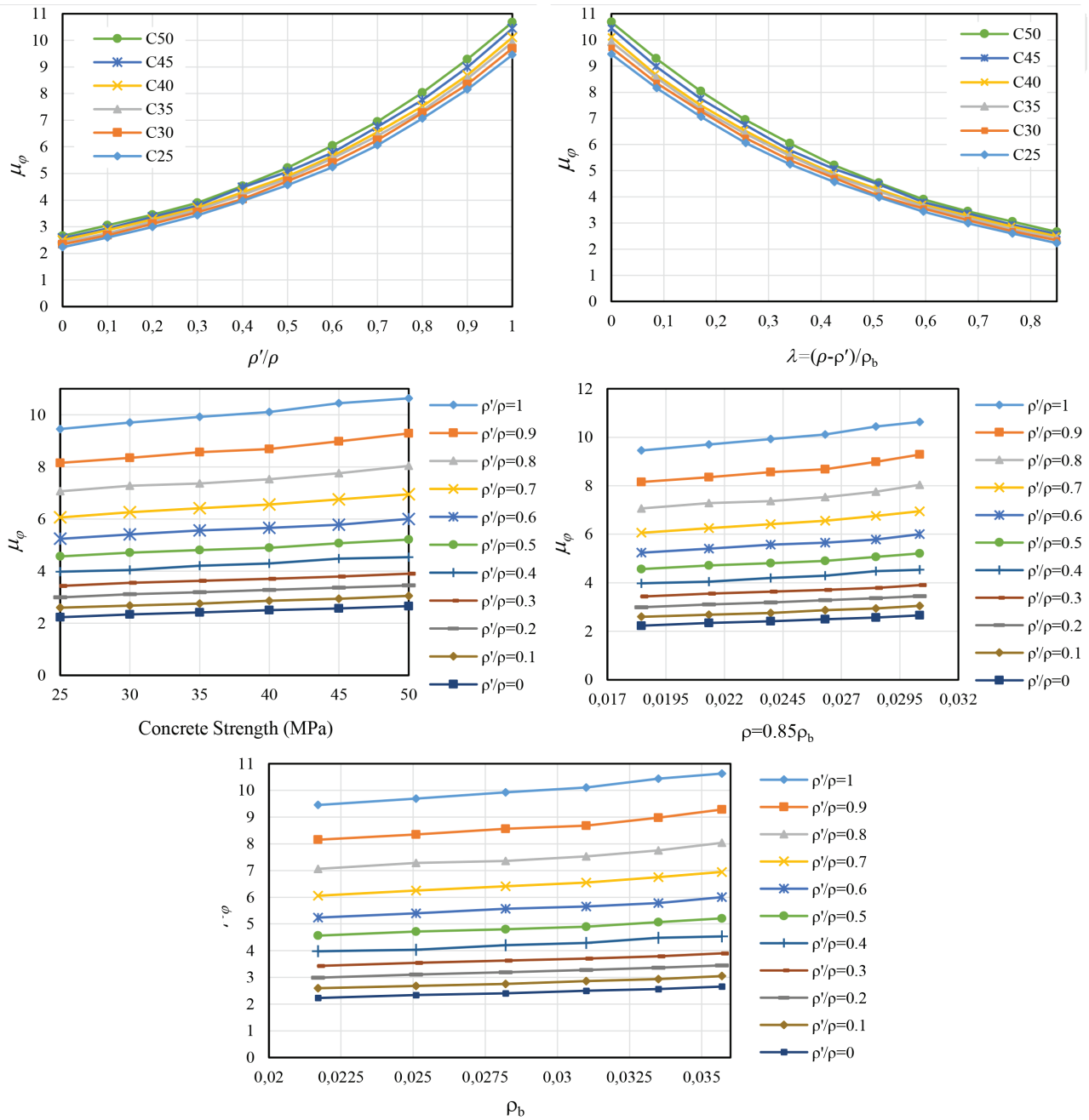


Fig. 8 Effect of different parameters on the curvature ductility

The results of the numerical analyses for  $f_{yk} = 420$  MPa,  $f_{yk} = 25$ MPa to 50MPa, and  $\rho'/\rho = 0$  to 1 indicate that the curvature ductility increases as  $\rho'/\rho$  increases for the doubly-reinforced beam sections. The curvature ductility decreases as  $\lambda$  increases for the doubly-reinforced beam sections. A regression analysis is undertaken to identify the effect of  $\lambda$  on the curvature ductility using the results of the numerical analyses. The effect of  $\lambda$  on the curvature ductility is illustrated in Fig. 9, which shows that the proposed equation closely matches the numerical results of the curvature ductility. The  $\lambda$  has a pronounced effect on the curvature ductility. The results of the numerical analyses show that the curvature ductility decreases with an increase in  $\lambda$ , though not proportionally. Based on the numerical analysis results, the relations of the curvature ductility factor and parameter  $\lambda$  can be obtained by regression analysis as follows:

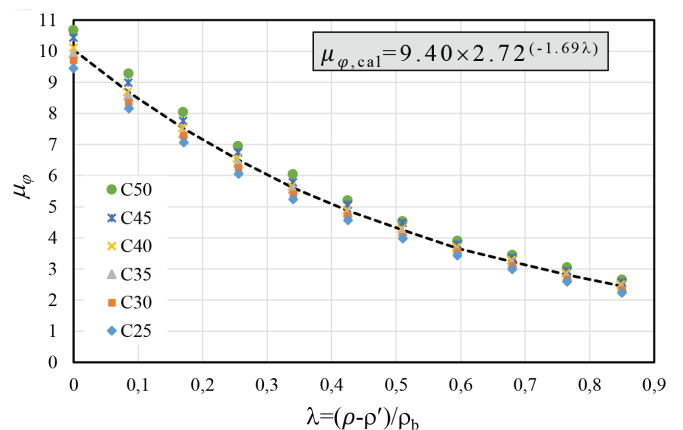


Fig. 9 Effect of parameter  $\lambda$  on the curvature ductility factor

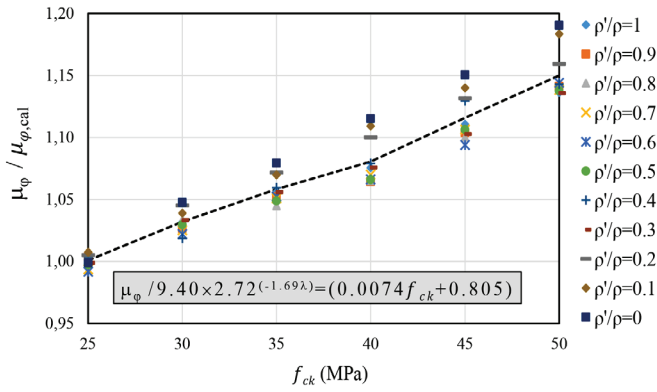


Fig. 10 Effect of  $f_{ck}$  on the ratio of curvature ductility factor to  $9.40 \times 2.72^{(-1.69\lambda)}$

$$\mu_{\phi,cal} = 9.40 \times 2.72^{(-1.69\lambda)} \quad (10)$$

Equation (10) clearly shows that the curvature ductility factor of doubly-reinforced beam sections can be expressed as a function of  $9.40 \times 2.72^{(-1.69\lambda)}$ . The effect of the concrete’s compressive strength on the ratio of the curvature ductility factor  $\mu_{\phi}$  to  $9.40 \times 2.72^{(-1.69\lambda)}$  is shown in Fig. 10. The numerical analysis results indicate that the curvature ductility factor increases with the increase in the concrete’s compressive strength. Through regression analysis, the relationship between the ratio of the curvature ductility factor  $\mu_{\phi}$  to  $9.40 \times 2.72^{(-1.69\lambda)}$  and the compression strength of the concrete and reinforcement can be obtained as follows:

$$\frac{\mu_{\phi}}{\mu_{\phi,cal}} = (0.0074 f_{ck} + 0.80) \quad (11)$$

Considering the effect of parameters such as the material strength and reinforcement ratio, the predictive equation of the curvature ductility factor in the doubly-reinforced beam sections can be offered based on the parametric study. The proposed curvature ductility ( $\mu_{\phi,prop}$ ) can be expressed as Equation (12). The effect of  $f_{ck}$ ,  $\rho'/\rho$  and  $\lambda$  on the ratio of the curvature ductility factor  $\mu_{\phi,prop}$  is given in Fig. 11.

$$\mu_{\phi,prop} = \left[ 9.40 \times 2.72^{(-1.69\lambda)} \times (0.0074 f_{ck} + 0.80) \right] \quad (12)$$

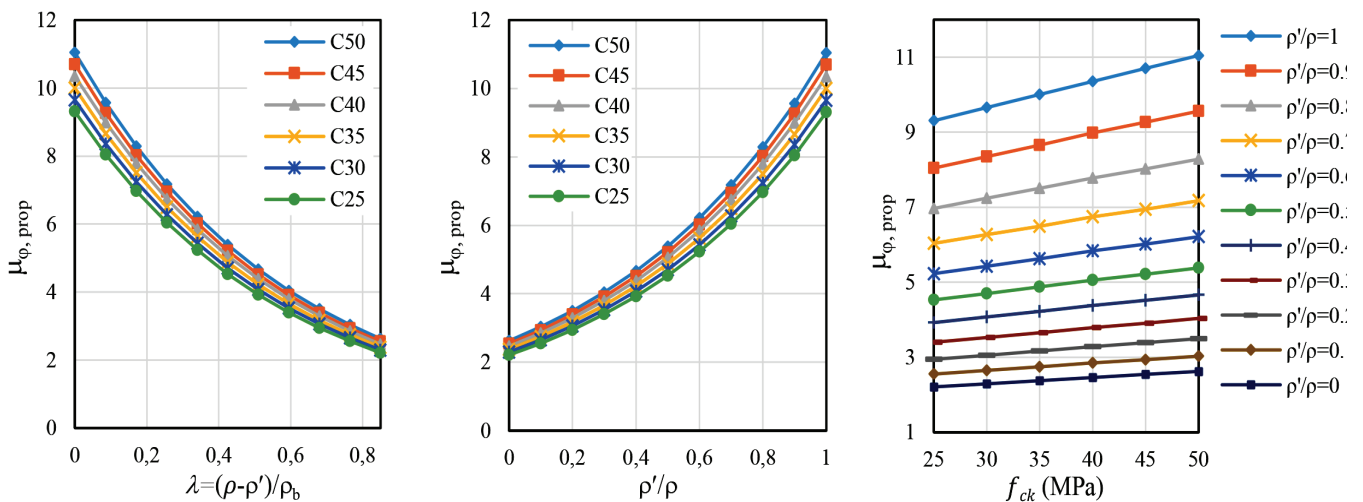


Fig. 11 Effect of  $f_{ck}$ ,  $\rho'/\rho$  and  $\lambda$  on the ratio of the curvature ductility factor  $\mu_{\phi,prop}$

### 5.5 Verification of the Proposed Predictive Equation for the Curvature Ductility Factor

In this part of the study, the flexural ductility of doubly-reinforced beam models designed with different concrete strengths and compression and tensile strength ratios according to the relations by the proposed curvature ductility equation (Equation 12) was calculated analytically. A comparison of the curvature ductility provided by the proposed Equation (12) with the numerical analysis results for the various  $f_{ck}$ ,  $\rho'/\rho$  and  $\lambda$  is given in Fig. 12. Fig. 13 shows a comparison of the curvature ductility factors obtained numerically with the proposed equation. The proposed predictions show excellent agreement as evident from the correlative coefficient  $R^2$ , which is well above 0.99. Also, the maximum mean value and the standard deviation for the ratio of the proposed curvature ductility factor obtained by Equation (12) to the numerical results are 1.02 and %2.139, respectively.

When examining the ratio of the results obtained from Equation (12) to the numerical results effected by the changes in  $f_{ck}$ ,  $\rho'/\rho$  and  $\lambda$ , it can be seen that the proposed predictions agree well with the numerical results within all the ranges of the parameters. The discrepancy between the numerical results and the results obtained from Equation (12) increases with the increasing  $f_{ck}$  and  $\rho'/\rho$  ratios and decreases with the increasing  $\lambda$  ratios. The curvature ductility obtained from the moment-curvature relations, the Kwan et al. (2002) equation, the Lee (2013) equation, the Pam et al. (2001a) equation, the Kwan and Ho (2010) equation, and the proposed predictive equation for the curvature ductility have been compared with the results of the numerical analyses. The relationship of the ductility factor variations with the degree of reinforcement and confining compression are given in Fig. 14. Fig. 15 shows the relations of the ductility factor variations with the  $\rho'/\rho$  and concrete strength.

According to the results obtained from the relations proposed for the curvature factor by Pam et al. (2001a) and Kwan et al. (2002), it can be seen that at a given concrete compressive strength, the ductility factor decreases with the tensile reinforcement ratio but increases with the compression reinforcement ratio. For constant  $\rho'/\rho$ , as the concrete’s compression strength increases, the ductility decreases. The ductility factor values calculated according to the minimum ductility factor specified by Kwan et al. (2002)

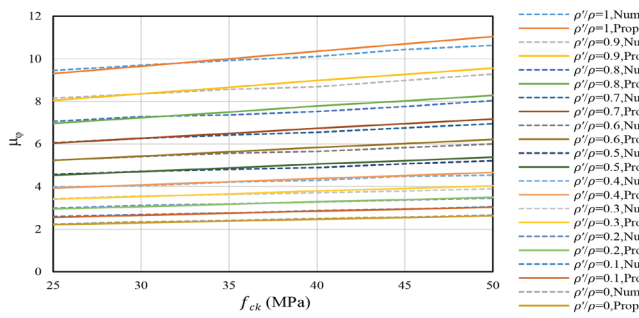


Fig. 12 Comparison of the curvature ductility for the proposed Equation (12) with the numerical analysis results for the various  $f_{ck}$ ,  $\rho'/\rho$ , and  $\lambda$ .

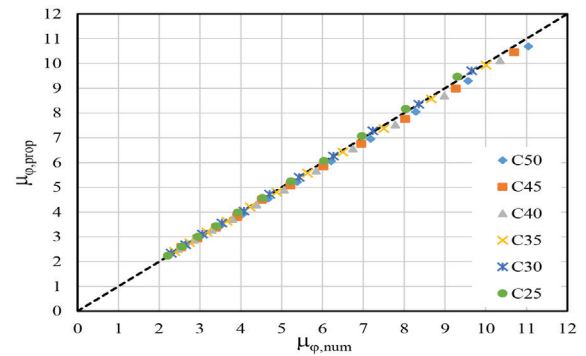


Fig. 13 Comparison of predicting the  $\mu_{\phi,prop}$  and numerical results

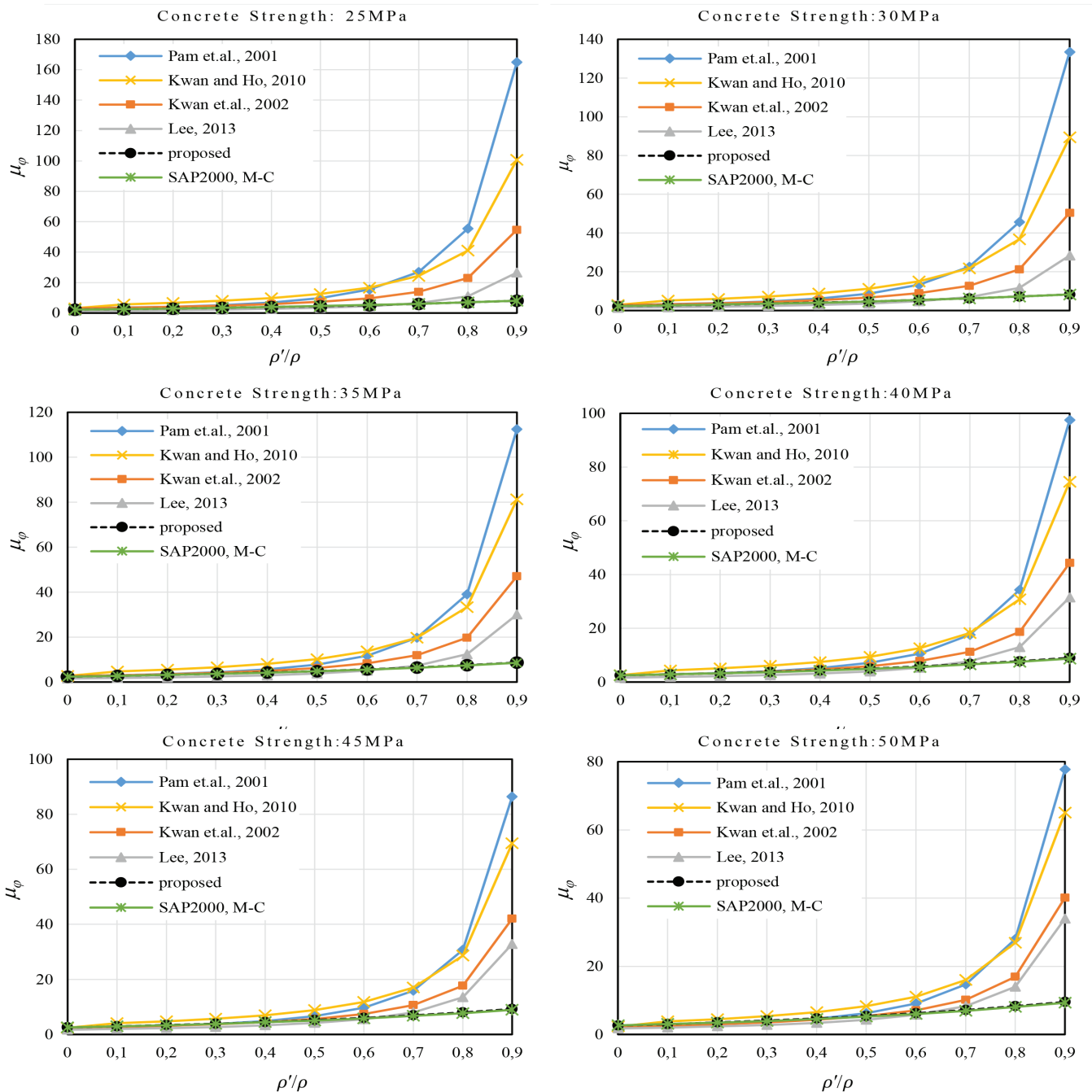
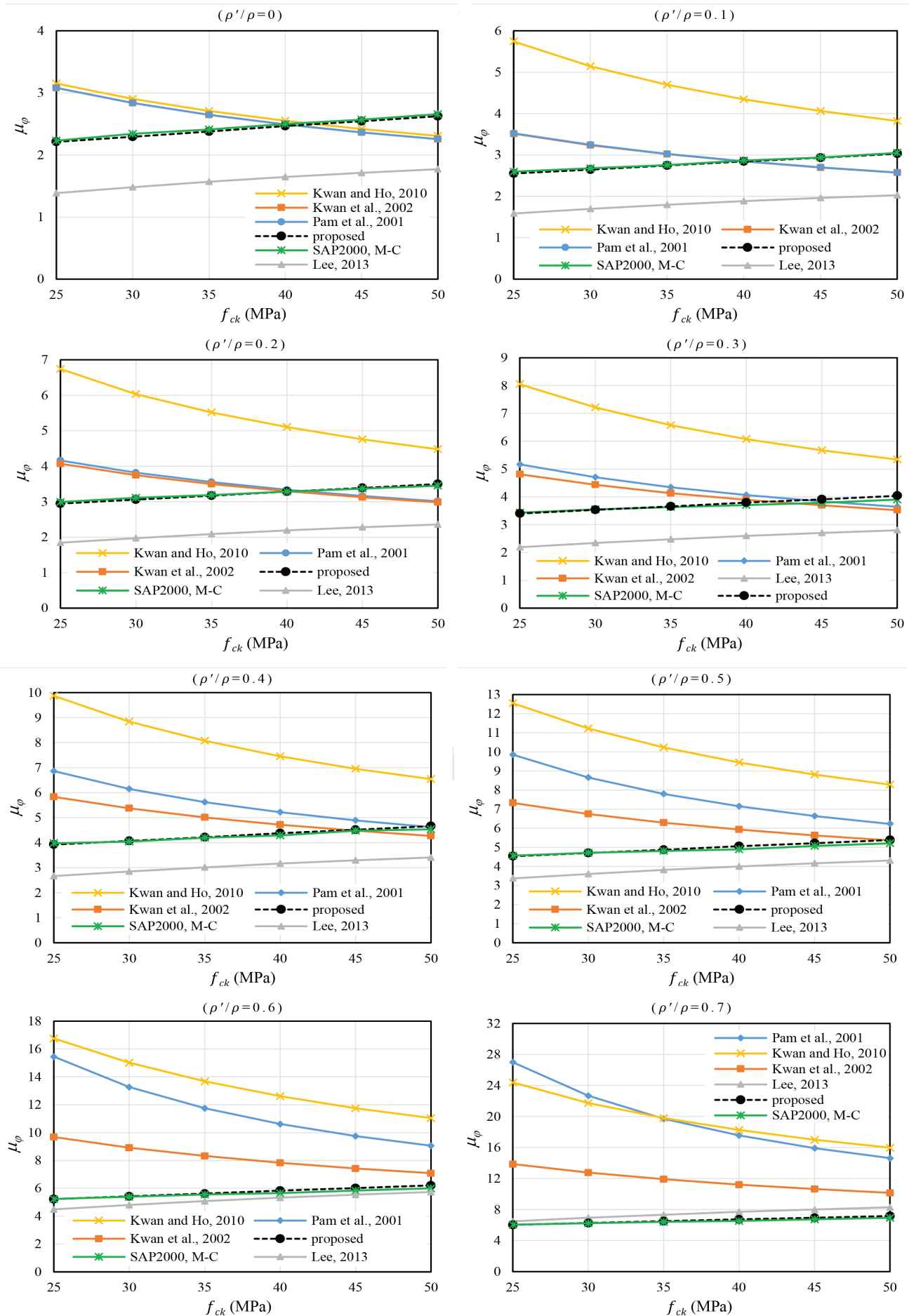


Fig. 14 Ductility factor ( $\mu_{\phi}$ ) of the doubly-reinforced beam sections versus the compression reinforcement ratio ( $\rho'/\rho$ )



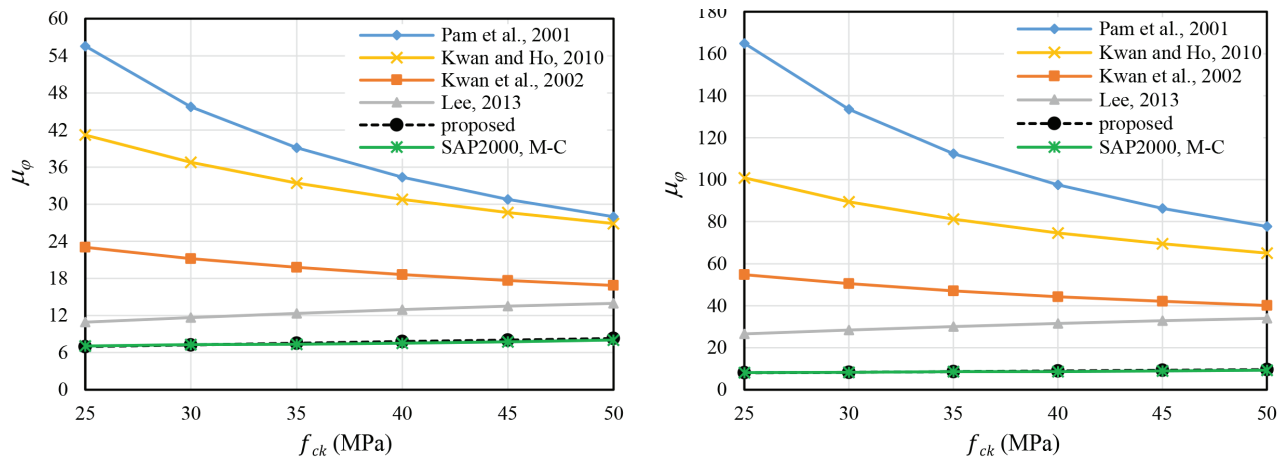


Fig. 15 Ductility factor ( $\mu_\phi$ ) of the doubly-reinforced beam sections versus the concrete's compression strength

yield small values according to the Pam et al. (2001a) equation. This is because the second term of the equation proposed by Pam et al. (2001a) is taken as 1.0. From the analysis of the results obtained from the relations proposed for the curvature factor proposed by Kwan and Ho (2010), the effect of the concrete's compressive strength has been found to be dependent on the ratios of the tensile and compression reinforcement, which determine the degree of reinforcement of the RC beams. It can be seen that as the concrete's compressive strength or tensile reinforcement ratio increases, the ductility decreases until it reaches a relatively low and constant value when the section becomes overly reinforced. It can also be seen that at the same degree of reinforcement ( $\lambda=0$ ), the ductility factor is lower at a higher concrete strength. This is because of the gradual reduction in material ductility as the concrete's compressive strength increases. However, at the same tensile reinforcement ratio, the ductility factor is lower at a higher concrete strength. The concrete's compressive strength increases, and the balanced reinforcement ratios also increase, thereby leading to a decrease in the degree of reinforcement and an increase in the ductility factor. From an analysis of the results obtained from the relations proposed for the curvature factor by Lee (2013), the curvature ductility factor in doubly-reinforced beam sections may be affected by the tensile reinforcement ratio, the compression reinforcement ratio, and the concrete's strength. This indicates that the ductility factor of doubly-reinforced beam sections increases with an increase in the compressive steel ratio. Under the same tensile reinforcement ratio, the ductility factor almost linearly decreases with the increase in the concrete's strength. The curvature ductility factor decreases with increasing  $\lambda$  ratios. It can be seen that the compression reinforcement ratio is the most effective factor. The effect of the concrete's strength and  $\lambda$  on the ratio of the curvature ductility factor  $\mu_{\phi,prop}$  according to the proposed predictive equation for curvature ductility is given in Figs. 12 and 13. The results of the analyses indicate that the curvature ductility decreases as  $\lambda$  increases for the doubly-reinforced beam sections. The curvature ductility increases as  $\rho'/\rho$  increases for the doubly-reinforced beam sections. The ductility increases with the increasing of the concrete's compressive strength concrete. The discrepancy between the numerical results and the results obtained from Equation (12) increases for the increase of  $f_{ck}$  and  $\rho'/\rho$ . The inconsistency between the results obtained from Equation (12) increases with the decreasing  $\lambda$  value. From a comparison of all the numerical results, almost the same curvature ductility values are obtained from the moment-curvature relations and the proposed equation (Equation 12).

For the ductility factor,  $f_{ck}$ ,  $\rho$ ,  $\rho'$  and  $\rho_b$  were considered as the main factors of the relations proposed by different researchers. In addition to these parameters, some researchers have taken into account the parameters of the stress of the compression reinforcement, the reinforcement yield strength, and the confining compression. In the relations suggested by the researchers, the limit values considered for the parameters are different. The parameters considered in the relations between Pam et al. (2001a) and Kwan et al. (2002) are the same, but the Kwan et al. (2002) relation suggested an economical formula to achieve the required ductility by modifying the Pam et al. (2001a) relation. Accordingly, it is natural that the values obtained for the two models are different. As can be seen from the results of the analysis, the values obtained from the Pam et al. (2001a) relation are higher than the value obtained from the Kwan et al. (2002) relation. The relationships proposed by the different researchers can be calculated up to  $\rho'/\rho = 0.9$ . In this study,  $\rho'/\rho = 0$  to  $\rho'/\rho = 1$  has been taken into consideration, but other researchers have considered  $\rho'/\rho = 0.75$  in their relations.

## 6 CONCLUSION

The flexural ductility of different parameters of concrete beams has been studied extensively by parametric studies according to the ductility factor relation suggested by various researchers and using a nonlinear moment-curvature analysis. They have proposed different relations for the ductility factor, which were discussed in detail in the Research Findings and Discussion Section, where the results obtained from these relations differ from each other. The results are different because the various researchers use factors such as different regulations, different material properties, different parameters, and different limit values for the tensile and compression reinforcement ratios. Based on the results of the numerical analyses, a simple equation is proposed for the prediction of the curvature ductility considering  $\lambda$  and the concrete's compressive strength. The proposed predictive Equation (12) is derived based on the results of sections with the concrete's strength ( $f_{ck}$ ) from 25MPa to 50MPa, the steel's yield strength  $f_y = 420$  MPa, the tensile reinforcement ratio from  $\rho = 0.85\rho_b$ , and the compression reinforcement ratio from  $\rho' = 0$  to  $\rho' = \rho$ . The proposed predictions show excellent agreement as evident from the correlative coefficients  $R^2$ , which is well above 0.99. Also, the maximum mean value and the standard deviation

for the ratio of the proposed curvature ductility factor obtained by Equation (12) to the numerical results are 1.0% and 2.1%, respectively. Based on the results of the numerical analysis, the proposed predictions for the curvature ductility factor, considering the concrete's strength and degree of reinforcement, is accurate to within an error of 2.19% for practical applications. The proposed

formula was verified by comparisons of its predictions with the numerical results and other predictions. The proposed formula offers fairly accurate and consistent predictions of the curvature ductility factor for doubly-reinforced beam sections. The curvature ductility can be conveniently and simply predicted using the proposed Equation (12).

## REFERENCES

- Adari, M. P. (2017)** *Influence of Curvature Ductility on Reinforced Concrete Beams under the Effect of Confinement*. International Journal for Research in Applied Science and Engineering Technology, 5, 246-255.
- Au, F.- Leung, C. C. Y. - Kwan, A. (2011)** *Flexural ductility and deformability of reinforced and prestressed concrete sections*. Computers and Concrete, 8, 473-489.
- Arslan, G. - Cihanli, E. (2010)** *Curvature ductility prediction of reinforced high-strength concrete beam sections*. Journal of Civil Engineering and Management, 16, 462–470.
- Bai, B. Z. Z. - Au, F. (2011)** *Flexural ductility design of high-strength concrete beams*. The Structural Design of Tall Special Buildings, 22, 521-542.
- CEB-FIP. (2010)** Fib Model Code for Concrete Structures.
- Debernardi, P. G. - Taliano, M. (2002)** *On evaluation of rotation capacity for reinforced concrete beams*. ACI Structural Journal, 99, 360-368.
- Dhakal, S. - Moustafa, M. (2019)** *Moment–curvature analysis for beams with advanced materials*, Software X, 9, 175-182.
- Eurocode 2. (2004)** Design of Concrete Structures - Part 1: General Rules and Rules for Buildings, Brussels, EN 1992-1-1 (2004).
- Jang, I. Y.- Park, H. G. - Kim, S. S. (2008)** *On the ductility of high-strength concrete beams*. International Journal of Computing Science and Mathematics, 2, 115-122.
- Haytham, B. - Amar, K. (2017)** *Curvature Ductility of High Strength Concrete Beams*. Journal of Materials and Engineering Structures, 4, 155-167.
- Ho, J. C. M.- Kwan, A. - Pam, H. J. (2004)** *Minimum flexural ductility design of high strength concrete beams*. Magazine of Concrete Research, 56, 13-22.
- Kwan, A. - Ho, J. C. M. (2010)** *Ductility design of high-strength concrete beams and columns*, Advances in Structural Engineering, 13, 651-664.
- Kwan, A. K. H.- Ho, J. C. M. - Pam, H. J. (2002)** *Flexural strength and ductility of reinforced concrete beams*. Proceedings of the Institution of Civil Engineers - Structures and Buildings, 152, 361-369.
- Liew, A.- Gardner, L. - Block, P. (2017)** *Moment-Curvature-Thrust Relationships for Beam- Columns*, Structures, 11, 146-154.
- Lee, H. J. (2013)** *Predictions of curvature ductility factor of doubly-reinforced concrete beams with high strength materials*. Computers and Concrete, 16, 831-850.
- Lam, J. Y. K.- Ho, J. C. M. - Kwan, A. (2009a)** *Maximum axial load level and minimum confinement for limited ductility design of concrete columns*. Computers and Concrete, 6, 357-376.
- Lam, J. Y. K.- Ho, J. C. M. - Kwan, A. K. H. (2009b)** *Flexural ductility of high-strength concrete columns with minimal confinement*, Materials and Structures, 42, 909-921.
- Pam, H. J.- Kwan, A. - Ho, J. C. M. (2001a)** *Post-peak behavior and flexural ductility of doubly-reinforced normal- and high-strength concrete beams*. Structural Engineering and Mechanics, 12, 459-474.
- Pam, H. J.- Kwan, A. - Islam, M. S. (2001b)** *Flexural strength and ductility of reinforced normal- and high-strength concrete beams*. Proceedings, Institution of Civil Engineers, Structures and Buildings, 146, 381-389.
- Pecce, M. - Fabbrocino, G. (1999)** *Plastic rotation capacity of beams in normal and high- performance concrete*. ACI Structural Journal, 96, 290-296.
- Park, R. - Paulay, T. (1975)** *Reinforced Concrete Structures*. Wiley, NY, U.S.A: 800, 1975.
- Rashid, M. A. - Mansur, M. A. (2005)** *Reinforced high-strength concrete beams in flexure*, ACI Structural Journal, 102, 462-471.
- Simão, P. D.- Barros, H. - Ferreira, C. C. (2016)** *Lossed-form moment-curvature relations for reinforced concrete cross sections under bending moment and axial force*. Engineering Structures, 129, 67-80.
- SAP2000**. Structural Software for Analysis and Design. Computers and Structures, Inc, USA.
- TBEC. (2018)** Specifications for Building Design Under Earthquake Effects. Turkish Building Earthquake Code, Ministry of Public Works and Housing, Ankara.
- TS500. (2000)** Requirements for Design and Construction of Reinforced Concrete Structures”, Turkish Standards Institute, Ankara, Turkey.
- Zareef, M. A. E. - Madawy, M. E. E. (2018)** *Effect of glass-fiber rods on the ductile behavior of reinforced concrete beams*. Alexandria Engineering Journal, 57, 4071-4079.